 Nucleic Acids Research, 1998, Vol. 26, No. 5 **1301–1308**

Probing structural elements in RNA using engineered disulfide cross-links

Emily J. Maglott and Gary D. Glick*

Department of Chemistry, University of Michigan, Ann Arbor, MI 48109-1055, USA

Received October 24, 1997; Revised and Accepted January 13, 1998

ABSTRACT

Three analogs of unmodified yeast tRNA^{Phe}, each possessing a single disulfide cross-link, have been designed and synthesized. One cross-link is between G1 and C72 in the amino acid acceptor stem, a second cross-link is in the central D region of yeast tRNA^{Phe} between C11 and C25 and the third cross-link bridges U16 and C60 at the D loop/T loop interface. Air oxidation to form the cross-links is quantitative and analysis of the cross-linked products by native and denaturing PAGE, RNase T1 mapping, Pb(II) cleavage, UV cross-linking and thermal denaturation demonstrates that the disulfide bridges do not alter folding of the modified tRNAs relative to the parent sequence. The finding that cross-link formation between thiol-derivatized residues correlates with the position of these groups in the crystal structure of native yeast tRNA^{Phe} and that the modifications do not significantly perturb native structure suggests that this methodology should be applicable to the study of RNA structure, conformational dynamics and folding pathways.

INTRODUCTION

The notion that structure is intimately coupled to function is an underlying tenet in contemporary biology. Proteins have been studied most extensively in this regard, primarily because there exists a wealth of methods to synthesize and characterize the structure and folding of polypeptides (1). For other biological macromolecules like RNA analogous structure–function relationships can also exist (2). RNA also bears other similarities to proteins in that both display a rich diversity of tertiary structure (3) and both proteins and RNA are believed to fold along discrete pathways (4). Our understanding of RNA structure and folding, however, lags behind that of proteins. One reason for this discrepancy is that high resolution RNA structures and straightforward methods to study RNA folding are only just emerging (5). Yet the similarities between these two classes of macromolecules raise the possibility of applying the methods and conceptual framework developed for examining proteins to the study of RNA (6).

One particularly useful technique both for stabilizing proteins and for probing protein function, structure, folding and dynamics is to generate cysteine mutants capable of forming disulfide cross-links and to use the disulfide bond as a reporter (7,8). At present there also exists a considerable body of research on the synthesis of disulfide cross-linked DNA oligomers (9–21). Aside from using the topological constraint imposed by the disulfide bond to stabilize ground state geometry (9–15), disulfide cross-links have been used to trap and isolate non-ground state DNA structures (16–18) and to examine the structural and energetic consequences of induced fit in both protein–DNA (19,20) and DNA–DNA systems (21). Building on this chemistry, we demonstrated the first example of site-specific incorporation of disulfide cross-links within RNA (22). In particular, we showed that disulfide cross-links can be used to stabilize RNA secondary structures (22) and to examine the solution conformation of larger RNAs (23). More recently disulfide cross-links have been employed to investigate the solution conformation of the hammerhead ribozyme (24), to stabilize a small RNA hairpin (25) and to examine domain motions in a 310 nt long group I ribozyme (26).

While recent work has shown that disulfide cross-links can be incorporated into RNA, the design of cross-links spanning complex regions of tertiary structure has not yet been demonstrated. Furthermore, the structural and thermodynamic consequences of constraining RNAs other than small hairpins/duplexes (27) has not yet been addressed in any detail. Such data are clearly a prerequisite for application of the disulfide cross-linking method in studies of RNA structure and function. As a first step in addressing these issues we have mapped the solution structure of three regions in tRNA^{Phe} from yeast (lacking the post-transcriptionally modified bases) using disulfide cross-links. We find that within the resolution of the chemical, enzymatic and thermal denaturation experiments performed our cross-links do not appear to perturb tertiary structure, even when the cross-link bridges an intricate region of tertiary structure, like the D loop/T loop interface. These results clearly demonstrate the utility of disulfide cross-links as a useful probe of RNA structure and should open the way for the general use of this method in structural and functional studies of ribonucleic acids.

MATERIALS AND METHODS

Nucleoside synthesis

The general synthetic and analytical protocols used here are those described by Goodwin *et al.* (23). Yields refer to chromatographically and spectroscopically homogeneous materials. Full compound characterization is in the supplementary material available on NAR Online. These data are also available in electronic form by contacting the corresponding author (gglick@umich.edu).

*To whom correspondence should be addressed. Tel: +1 313 764 4548; Fax: +1 313 763 2307; Email: gglick@umich.edu

See supplementary material available in NAR Online.

3′,5′-*O*-(Tetraisopropyldisiloxane-1,3-diyl)-2′-*O*-(2,3-dihydroxy proyl)uridine (1)

3′,5′-*O*-(Tetraisopropyldisiloxane-1,3-diyl)-2′-*O*-allyluridine (1.61 g, 3.06 mmol) (28) was dissolved in a mixture of acetone:H_2O (30 ml, 6:1). 4-Methylmorpholine *N*-oxide (394 mg, 3.4 mmol, 1.1 equiv.) and OsO_4 (7.7 mg, 0.03 mmol, 0.01 equiv.) were added. After stirring in the dark for 3 h the osmium salts were precipitated with saturated $NaHSO_4$ (2 ml) and the mixture was filtered through Celite. The solvent was evaporated *in vacuo* to afford **1** as a white foam (1.77 g, 100% yield). ^{13}C NMR (75 MHz, $CDCl_3$) δ 13.07–13.90 [Si*C*H(CH_3)$_2$], 17.18–17.82 [SiCH(*C*H$_3$)$_2$], 59.66 (5′), 68.58 (3′), 70.94 [CH_2CH(OH)*C*H$_2$OH], 74.20 [*C*H$_2$CH(OH)CH$_2$OH], 82.22 (4′), 83.99 [CH$_2$*C*H(OH)CH$_2$OH], 89.43 (1′), 89.67 (2′), 102.33 (5), 139.24 (6), 150.82 (2), 163.33 (4).

3′,5′-*O*-(Tetraisopropyldisiloxane-1,3-diyl)-2′-*O*-(ethanal)-uridine (2)

Compound **1** (437 mg, 0.8 mmol) was dissolved in 1,4-dioxane: H_2O (7.8 ml, 3:1) and $NaIO_4$ (209 mg, 1.0 mmol, 1.25 equiv.) was added. The reaction was stirred in the dark for 6 h, then diluted with Et_2O, filtered, washed with saturated $NaHCO_3$, dried over Na_2SO_4 and concentrated *in vacuo* to afford **2** as a pale yellow foam (400 mg, 97% yield). ^{13}C NMR (75 MHz, $CDCl_3$) δ 12.87–13.82 [Si*C*H(CH_3)$_2$], 17.11–17.78 [SiCH(*C*H$_3$)$_2$], 59.64 (5′), 68.95 (3′), 76.62 (O*C*H$_2$CHO), 82.00 (4′), 83.85 (2′), 89.32 (1′), 102.03 (5), 139.41 (6), 150.18 (2), 163.21 (4), 200.35 (OCH$_2$*C*HO).

3′,5′-*O*-(Tetraisopropyldisiloxane-1,3-diyl)-2′-*O*-(2-hydroxy-ethyl)uridine (3)

Compound **2** (470 mg, 0.9 mmol) was dissolved in CH_3OH (7.4 ml); $NaBH_4$ (16 mg, 0.4 mmol, 0.48 equiv.) was added and the mixture was stirred overnight under N_2. The mixture was diluted with Et_2O, washed once with saturated $NaHCO_3$ (aqueous) and twice with brine. The combined organic layers were dried over Na_2SO_4, filtered and evaporated *in vacuo* to afford **3** as a white foam (464 mg, 98% yield). ^{13}C NMR (90 MHz, $CDCl_3$) δ 12.73–13.62 [Si*C*H(CH_3)$_2$], 16.97–17.65 [SiCH(*C*H$_3$)$_2$], 59.46 (5′), 61.78 (OCH$_2$*C*H$_2$OH), 68.37 (3′), 73.20 (O*C*H$_2$CH$_2$OH), 81.99 (4′), 83.04 (2′), 89.62 (1′), 101.99 (5), 139.38 (6), 150.58 (2), 163.80 (4). MS (CI, CH4) *m*/*z* 531 (M^+).

3′,5′-*O*-(Tetraisopropyldisiloxane-1,3-diyl)-2′-*O*-(ethyl-2-methyl sulfonate)uridine (4)

Compound **3** (138 mg, 0.3 mmol) was dissolved in a mixture of CH_2Cl_2 (2.6 ml) and pyridine (0.21 ml) and cooled to 0°C. Methanesulfonyl chloride (28 µl, 0.4 mmol, 14 equiv.) was added dropwise with stirring under N_2 and the reaction was allowed to warm to room temperature over 18 h. The mixture was diluted with CH_2Cl_2 and washed once with saturated $NaHCO_3$ (aqueous). The organic layer was dried over Na_2SO_4, filtered, evaporated *in vacuo* and the residue purified by flash chromatography with CH_2Cl_2:acetone (17:3) as eluent to afford **4** as a white foam (133 mg, 84% yield). ^{13}C NMR (75 MHz, $CDCl_3$) δ 12.85–13.74 [[Si*C*H(CH_3)$_2$], 17.07–17.73 [SiCH(*C*H$_3$)$_2$], 38.00 (S*C*H3), 59.59 (5′), 68.63 (3′), 69.29 (OCH$_2$*C*H$_2$OMs), 69.44 (O*C*H$_2$CH$_2$OMs), 81.93 (4′), 83.27 (2′), 88.96 (1′), 101.97 (5), 139.38 (6), 150.33 (2), 163.60 (4).

3′,5′-*O*-(Tetraisopropyldisiloxane-1,3-diyl)-2′-*O*-(thiobenzoyl-ethyl)uridine (5)

Compound **4** (552 mg, 0.9 mmol) was dissolved in a mixture of DMF (3.6 ml) and Et_3N (1.3 ml, 9.1 mmol, 10.0 equiv.) and thiobenzoic acid (0.21 ml, 1.8 mmol, 2 equiv.) was added. After stirring overnight under N_2 the mixture was diluted with Et_2O, washed once with saturated $NaHCO_3$ (aqueous) and twice with brine. The combined organic extracts were dried over Na_2SO_4, filtered, concentrated *in vacuo* and the residue purified by flash chromatography (step gradient of 6–20% acetone in CH_2Cl_2) to afford **5** as a white foam (472 mg, 80% yield). ^{13}C NMR (90 MHz, $CDCl_3$) δ 12.71–13.62 [Si*C*H(CH_3)$_2$], 17.00–17.70 [SiCH(*C*H$_3$)$_2$], 29.16 (OCH$_2$*C*H$_2$S), 59.57 (5′), 68.45 (3′), 70.12 (O*C*H$_2$CH$_2$S), 81.88 (4′), 82.60 (2′), 89.34 (1′), 101.71 (5), 127.45, 128.74, 133.53, 137.18 (Ar), 139.73 (6), 150.14 (2), 163.92 (4), 191.67 (CO).

2′-*O*-(Thiobenzoylethyl)uridine (6)

Compound **5** (472 mg, 0.7 mmol) was dissolved in CH_3CN (5.8 ml) and HF (aqueous) (1.3 ml, 48%) was added. After stirring for 4 h the mixture was diluted with EtOAc and washed once with H_2O. The organic layer was dried over Na_2SO_4, filtered and evaporated *in vacuo* to afford **6** as a white foam (327 mg, 100% yield). ^{13}C NMR (90 MHz, CD_3OD) δ 29.70 (OCH$_2$*C*H$_2$S), 61.77 (5′), 70.01 (3′), 70.65 (O*C*H$_2$CH$_2$S), 83.80 (4′), 86.26 (2′), 89.31 (1′), 102.74 (5), 128.27, 130.04, 134.94, 138.30 (Ar), 142.58 (6), 152.35 (2), 166.36 (4), 193.18 (CO). MS (CI, CH4) *m*/*z* 409 (M^++1).

5′-*O*-(4,4′-Dimethoxytrityl)-2′-*O*-(thiobenzoylethyl)uridine (7)

Compound **6** (277 mg, 0.7 mmol) was dissolved in a mixture of DMF (2.7 ml) and pyridine (82 µl, 1.0 mmol, 1.5 equiv.); 4,4′-dimethoxytrityl chloride (280 mg, 0.8 mmol, 1.2 equiv.) and 4-dimethylaminopyridine (54 mg, 0.4 mmol, 0.65 equiv.) were added. The reaction was stirred overnight under N_2 and then diluted with CH_2Cl_2. The solution was washed once with saturated $NaHCO_3$ (aqueous) and twice with brine and the combined organic extracts were dried over Na_2SO_4, filtered and concentrated *in vacuo*. The residue was purified by flash chromatography with CH_2Cl_2:CH_3OH (48:1) as eluent to afford **7** as a yellow foam (302 mg, 63% yield). ^{13}C NMR (90 MHz, CD_3CN) δ 17.03 (OCH$_2$*C*H$_2$S), 56.02 (O*C*H$_3$), 63.11 (5′), 69.86 (3′), 70.28 (O*C*H$_2$CH$_2$S), 83.21 (2′), 84.04 (4′), 87.65 [O*C*(Ph)$_3$], 88.68 (1′), 102.55 (5), 114.24 (Ar), 128.06, 129.02, 129.14, 129,98, 131.17, 131.64, 134.81, 136.49, 136.73, 137.89 (Ar), 141.17 (6), 145.87 (Ar), 151.41 (2), 159.86 (Ar), 161.07 (4), 192.35 [S*C*(O)Ph]. MS (CI, CH4) *m*/*z* 710 (M^+).

5′-*O*-(4,4′-Dimethoxytrityl)-2′-*O*-(ethyl)uridine t-butyl disulfide (8)

Compound **7** (293 mg, 0.4 mmol) was dissolved in THF:CH_3OH (3.3 ml, 1:1) and LiOH (26 mg, 0.6 mmol, 1.5 equiv.) was added. After stirring for 2 min 1-(t-butylthio)-1,2-hydrazinecarbox-morpholide (164 mg, 0.5 mmol, 1.2 equiv.) (29) was added and the mixture stirred for an additional 10 min under N_2. The solution was diluted with CH_2Cl_2, washed with 1 M citric acid,

saturated $NaHCO_3$ (aqueous) and brine. The organic layer was dried over Na_2SO_4, filtered and evaporated *in vacuo*. The residue was purified by flash chromatography eluting with CH_2Cl_2:CH_3OH (49:1) to afford **8** as a white foam (285 mg, 100% yield). ^{13}C NMR (90 MHz, acetone-d_6) δ 29.28–30.56 [acetone, C(*C*H_3)$_3$], 40.79 (OCH$_2$*C*H$_2$S), 48.32 [*C*(CH$_3$)$_3$], 55.61 (O*C*H$_3$), 63.15 (5′), 69.94 (3′), 70.16 (O*C*H$_2$CH$_2$S), 83.30 (2′), 84.03 (4′), 87.58 (Ar), 88.75 (1′), 102.41 (5), 114.09, 127.83, 128.82, 129.13, 131.14, 136.37, 136.67 (Ar), 140.88 (6), 145.93 (Ar), 151.29 (2), 159.80 (Ar), 163.58 (4). FAB MS (3-NBA) *m/z* 695 (M^++1).

3′-*O*-(*N*,*N*-Diisopropyl-β-cyanoethyl-phosphoramidite)-5′-*O*-(4,4′-dimethoxytrityl)-2′-*O*-(ethyl)uridine t-butyl disulfide (9)

Compound **8** (49 mg, 0.07 mmol) was dissolved in CH_2Cl_2 (0.28 ml) containing *N*,*N*-diisopropylethylamine (62 µl, 0.4 mmol, 5 equiv.) and cooled to 0°C. Chloro-*N*,*N*-diisopropylamine-β-cyanoethyl phosphine (24 µl, 0.1 mmol, 1.5 equiv.) was added dropwise and the mixture was stirred for 2 h under N_2. The solution was diluted with CH_3OH, concentrated *in vacuo* and the residue was purified by flash chromatography with petroleum ether:acetone (19:6) as eluent to afford **9** as a white foam (49 mg, 78% yield). ^{13}C NMR (75 MHz, acetone-d_6) δ (two diastereomers) 20.96 [N*C*H(CH$_3$)$_2$], 25.02–25.32 [NCH(*C*H$_3$)$_2$], 29.14–30.68 [acetone, SSC(*C*H$_3$)$_3$], 41.17 (OCH$_2$*C*H$_2$S), 44.07, 44.24 (*C*H$_2$CN), 48.27 [SS*C*(CH$_3$)$_3$], 55.68 (O*C*H$_3$), 59.25–59.92 (POCH$_2$), 62.72, 63.00 (5′), 70.27, 70.41 (O*C*H$_2$CH$_2$S), 71.30, 71.48 (3′), 82.11, 82.81 (2′), 83.14–83.41 (4′), 87.78 (Ar), 89.04, 89.29 (1′), 102.53, 102.59 (5), 114.10 (Ar), 118.81, 118.96 (CN), 127.80, 128.72, 129.19, 131.15, 131.53, 136.27, 136.35, 136.45 (Ar), 140.65, 140.72 (6), 145.68, 145.75 (Ar), 151.21 (2), 159.80 (Ar), 163.37 (4). ^{31}P NMR (202 MHz, CD_3CN) δ 147.44, 146.90. FAB MS (3-NBA) *m/z* 895 (M^++1). Analysis: calculated for $C_{45}H_{59}N_4O_9PS_2$, C 60.38, H 6.64, N 6.26; found, C 60.59, H 6.59, N 5.95.

RNA synthesis and analysis

The general procedures for synthesis and purification were performed as previously described (23). Site **I** was synthesized without the last four bases at the 3′-end. All other sequences were synthesized on 1000 Å deoxyadenosine controlled pore glass. Disulfide cross-link formation was also conducted as previously described (23). Briefly, each t-butyl disulfide-modified tRNA (~3 OD_{260} U, 130 µg, 5 nmol) was reduced with DTT (54 µg, 200 equiv./disulfide) at 25°C for 12 h in phosphate buffer (50 µl, 100 mM Na_2HPO_4, pH 8.3). The DTT was removed by dialysis against phosphate buffer (3 l, 5 mM Na_2HPO_4, 5 mM NaCl, pH 7.0) at room temperature for 10 h. The tRNA was then diluted in the same phosphate buffer (pH 7.0) to a final concentration of 4 µM, heated to 70°C for 1 min and allowed to cool to ~40°C. At this time $MgCl_2$ (0.1 M) was added to a final [Mg^{2+}] of 5 mM and the solution was equilibrated at room temperature for 30 min. After adjusting the pH to 8.0 the reaction was stirred at room temperature exposed to air for 12 h, at which time cross-link formation was complete as determined by either analytical PAGE or by analysis with *N*-(4-(7-diethylamino-4-methylcoumarin-3-yl)phenyl)maleimide (30). The reaction mixture was either ethanol precipitated or dialyzed against TE buffer (3 l, 10 mM Tris–HCl, 1 mM EDTA, pH 8.0, 10 h) and stored at –20°C.

5′-^{32}P-End-labeling of each tRNA was performed using standard conditions as previously described (23). All footprinting experiments were analyzed on denaturing gels (15% polyacrylamide, 29:1 acrylamide:bisacrylamide, 8 M urea, 310 × 385 × 0.4 mm). Product bands were quantified using a Molecular Dynamics phosphorimager.

Native RNase T1 mapping was conducted using the methods described by Hall and Sampson (31) with the exception that only 1 µg unlabeled tRNA from brewer's yeast was used as carrier. The reactions were quenched by addition of water (20 µl), extracted twice with phenol to remove the protein and ethanol precipitated. For enzyme mapping reactions of disulfide cross-linked tRNAs the pellets were dissolved in buffer (10 µl, 20 mM Tris–HCl, 20 mM NaCl, 10 mM $MgCl_2$, 8.5 mM EDTA, pH 7.0), DTT (10 µl, 100 mM) was added and the reactions were incubated at 37°C for 1 h. The reductions were quenched with NaOAc (17 µl, 1.5 M, pH 5.5) and ethanol precipitated prior to electrophoresis.

Rates of Pb(II) autocleavage were measured as described by Han and Dervan (32). The fraction of Pb^{2+} cleavage product was determined for aliquots (5 µl) removed at the specified times during the first 8 min of incubation with Pb^{2+}. Reactions with disulfide cross-linked tRNAs were quenched with EDTA (5 µl, 167 mM) and treated with DTT as above. Rates were obtained from the slopes of plots of fraction of cleavage versus time. Rates of ultraviolet cross-link formation were obtained using the method of Behlen *et al.* (33) from quantification of the amount of cross-linked product formed over time during the first 5 min of exposure to 254 nm irradiation. UV spectra were measured and analyzed as previously described (23).

RESULTS AND DISCUSSION

Synthesis of RNA analogs possessing cross-links within complex regions of RNA tertiary structure is a challenging exercise in molecular design. In previous work we described the synthesis of two disulfide cross-linked tRNA analogs of yeast $tRNA^{Phe}$ (23). The first construct is a closed circular molecule produced by placing a cross-link at the terminus of the amino acid acceptor stem (**I**, Fig. 1A). The second tRNA possesses a disulfide cross-link between residues C11 and C25 and it was designed to constrain folding of the variable loop onto the D stem (**II**, Fig. 1B). Here we apply the principles used to design these constructs (i.e. avoiding disruption of interactions that stabilize secondary and tertiary structure) to the synthesis of a third disulfide cross-linked tRNA which is located in a very complex region of tertiary structure and probe in detail the solution structure of all three cross-linked tRNAs.

The characteristic L-shape of tRNA arises due to folding of the D-loop onto the T-loop. In the crystal structure of yeast $tRNA^{Phe}$ both U59 and C60 project out of the minor groove of the T-stem helix, permitting residue A58 to pair with U54 of the UUCG tetraloop. To form the third cross-linked tRNA we reasoned that replacing U16 and C60 with $\mathbf{U^{2'S}}$ and $\mathbf{C^{2'S}}$ respectively (**III**, Fig. 1C) would allow formation of a disulfide bond without interfering with any putative Mg^{2+} binding sites. A covalent cross-link that tethers the T- and D-loops would limit the range of motion of the two loops, thereby stabilizing the folded tRNA structure. Aside from producing a construct that is (kinetically and/or thermodynamically) resistant to denaturation, this construct could be used to investigate conformational changes that occur

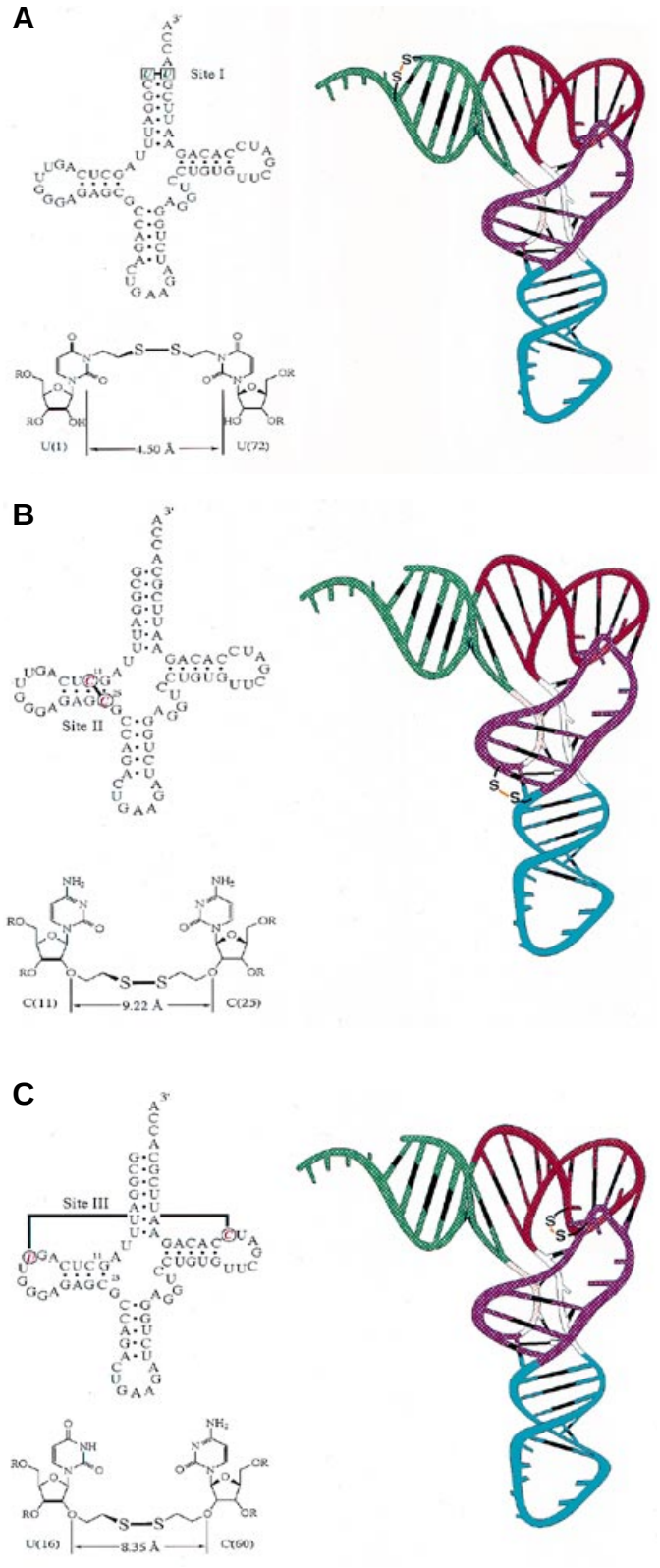

Figure 1. Yeast $tRNA^{Phe}$ crystal structure showing the locations of the cross-links. Green, aminoacyl acceptor stem; purple, dihydrouridine-stem and loop; blue, anticodon stem and loop; red, TΨC stem and loop. (**A**) Site **I**; (**B**) site **II**; (**C**) site **III**. The sequences containing the t-butyl disulfide-protected residues are designated $\mathbf{I_{tBu}}$, $\mathbf{II_{tBu}}$ and $\mathbf{III_{tBu}}$ for sites **I**, **II** and **III** respectively. The corresponding disulfide cross-linked sequences are designated $\mathbf{I_{XL}}$, $\mathbf{II_{XL}}$ and $\mathbf{III_{XL}}$.

upon amino acid charging, codon binding and interaction with ribosomes (34).

Monomer synthesis for the U16 and C60 cross-link

The synthesis of $\mathbf{U^{3S}}$ and $\mathbf{C^{2'S}}$ has been described previously (23) and preparation of protected $\mathbf{U^{2'S}}$ is shown in Scheme 1. Briefly, the allyl group of 3′,5′-*O*-(tetraisopropyldisiloxane-1,3-diyl)-2′-*O*-allyluridine (28) was selectively dihydroxylated using OsO_4. The vicinal diol was cleaved with $NaIO_4$ and the resulting aldehyde was reduced with $NaBH_4$ to afford saturated alcohol **3**. To introduce the thiol, **3** was activated as a mesylate and displacement with thiobenzoic acid afforded thioester **5**. Removal of the silyl protecting group was achieved with aqueous HF and the 5′-hydroxyl was protected as a 4,4′-dimethoxytrityl ether. Conversion of the thiobenzoyl group to the t-butyl mixed disulfide provided a masked thiol group that is stable to all solution conditions associated with solid phase synthesis, including deprotection and desilylation. Finally, activation of the 3′-hydroxyl as the *N*,*N*-diisopropyl-β-cyanoethyl phosphoramidite provided the desired monomer in a form suitable for solid phase RNA synthesis. These thiol-modified *N*,*N*-diisopropyl-β-cyanoethyl phosphoramidites are all stable as solutions in acetonitrile (50–55 mM) for at least 5 days at room temperature as determined by NMR.

RNA synthesis and cross-link formation

Solid phase RNA synthesis was conducted on a 1 µmol scale using A^{Bz}, C^{Bz}, G^{iBu} and U phosphoramidites with the 2′-hydroxyl groups protected as t-butyldimethylsilyl ethers (35). Coupling efficiencies for the alkylthiol-modified phosphoramidites were indistinguishable from those obtained using the corresponding parent nucleosides (>98.5%). Deprotection and desilylation of each tRNA was accomplished with anhydrous ethanolic ammonia and tetra-*n*-butylammonium fluoride (1 M in THF) respectively (35). The t-butyl disulfide-protected tRNA sequences were purified to single nucleotide resolution by denaturing polyacrylamide gel electrophoresis (PAGE). In general, 350 µg tRNA that is ≥98% pure as judged by ethidium staining of denaturing polyacrylamide gels could be obtained from one synthesis, which is among the most efficient chemical tRNA syntheses reported (36,37).

Disulfide cross-link formation was conducted by first reducing the t-butyl disulfide protecting groups on the requisite tRNA with a 200-fold excess of dithiothreitol (DTT) in a pH 8.3 buffer to liberate the free thiols. These conditions selectively reduce the mixed disulfide without degradation of the tRNA, as judged by denaturing PAGE. Because DTT co-precipitates with tRNA under standard ethanol precipitation conditions, dialysis was used to effect complete removal of the DTT. During dialysis, aliquots of the dialyzate were monitored with *N*-(4-(7-diethylamino-4-methylcoumarin-3-yl)phenyl)maleimide (30) to determine when all DTT was removed. This reagent was chosen because it selectively reacts with free thiols and the fluorescent adduct can be used to detect thiol concentrations as low as 0.5 µM, which is significantly more sensitive than Ellman's test for the presence of free thiol groups (38).

To oxidize the thiol groups the fully reduced tRNAs were first folded in the presence of Mg^{2+} (5 mM) and after adjusting the pH to 8.0 the solutions were stirred vigorously in air at room temperature. In general disulfide cross-link formation was conducted at tRNA concentrations of 1–4 µM to suppress

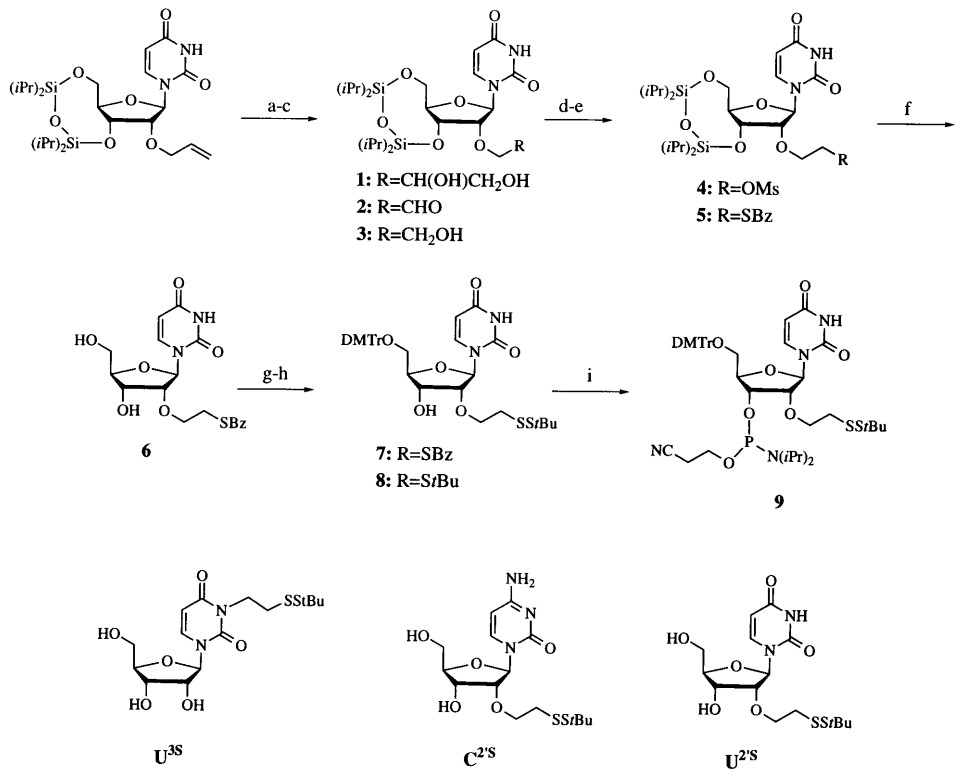

Scheme 1. (**a**) OsO_4 4-methylmorpholine *N*-oxide, acetone, H_2O (100%); (**b**) $NaIO_4$, *p*-dioxane, H_2O (97%); (**c**) $NaBH_4$, MeOH (98%); (**d**) methanesulfonylchloride, pyridine (84%); (**e**) thiobenzoic acid, Et_3N, DMF (80%); (**f**) HF (aqueous). CH_3CN (100%); (**g**) DMTrCl, pyr, DMF, DMAP (63%); (**h**) l-t-butylthio-1,2-hydrazinedicarboxmorpholide, LiOH, MeOH, THF (74%); (**i**) chloro-*N*-*N*-diisopropylamine-β-cyanoethylphosphine, *N*-*N*-diisopropylethylamine, CH_2Cl_2 (78%).

formation of intermolecular disulfide bonds. Under these conditions air oxidation affords complete conversion of each reduced sequence in <12 h to one product of slower mobility (39) than the corresponding t-butyl disulfide tRNA precursor on 15% denaturing polyacrylamide gels (e.g. $\mathbf{I_{XL}}$ and $\mathbf{III_{XL}}$ migrate 5 cm less than $\mathbf{I_{tBu}}$ and $\mathbf{III_{tBu}}$ and $\mathbf{II_{XL}}$ migrates 1 cm less than $\mathbf{II_{tBu}}$; for a representative gel see 23). In some cases cross-link formation was also monitored by the decrease in free thiol concentration as determined using the fluorescence assay described above.

Treatment of each of the cross-linked products with DTT results in products that co-migrate with the corresponding precursor t-butyl disulfide-modified tRNAs on both native and denaturing gels, indicating that a disulfide bond is present in the oxidation product (mobility differences between thiol- and t-butyl disulfide-containing tRNAs cannot be detected by PAGE). Furthermore, each disulfide cross-linked tRNA migrates with the same apparent molecular weight as unmodified yeast $tRNA^{Phe}$ on native polyacrylamide gels, demonstrating that the cross-links are intramolecular (data not shown). The ability to form each disulfide cross-link in quantitative isolated yields compares favorably with yields of other disulfide cross-linked RNAs [e.g. 66% isolated yield of a disulfide cross-linked RNA hairpin (25) and a 15% overall yield of disulfide cross-linked hammerhead ribozyme (24)]. The fact that each cross-link forms in high yield suggests that the disulfide bonds are not strained and provides further evidence that the solution structure of unmodified yeast $tRNA^{Phe}$ is very similar to the conformation of yeast $tRNA^{Phe}$ observed in the crystal.

Solution structure mapping

To probe the effect of our modifications on native tertiary structure, the conformation of the disulfide cross-linked and t-butyl disulfide-protected tRNAs were examined by chemical and enzymatic footprinting under conditions where unmodified yeast $tRNA^{Phe}$ is correctly folded (40). The most distinct feature of tRNA tertiary structure involves the D-loop/T-loop interaction at the 'hinge region'. Assays that probe the structure in this region of the tRNA are good indicators of correct tertiary folding. Most notably, the rate of both Pb(II)-induced autocleavage (32,40) and pyrimidine photodimerization (33) are sensitive assays of local structure at the hinge region, as well as of the overall conformation of the tRNA. Prior to these experiments, however, we probed the gross tertiary structure throughout the entire tRNA by RNase T1 footprinting (41).

RNase T1 cleaves 3′ of single-stranded guanosines. There are 23 guanosine residues in unmodified yeast $tRNA^{Phe}$, 10 of which are located in the loop regions of the cloverleaf secondary structure. Four of these residues are not involved in tertiary hydrogen bonding interactions and therefore should be accessible to cleavage by the enzyme: G20 in the D loop, G34 and G37 in the anticodon loop and G57 in the T loop. Several guanosine residues in both single- and double-stranded regions of the tertiary structure of unmodified yeast $tRNA^{Phe}$ are in close proximity to the modifications we have introduced. The presence or absence of expected cleavages at these and other residues should report on the local structure surrounding the cross-link.

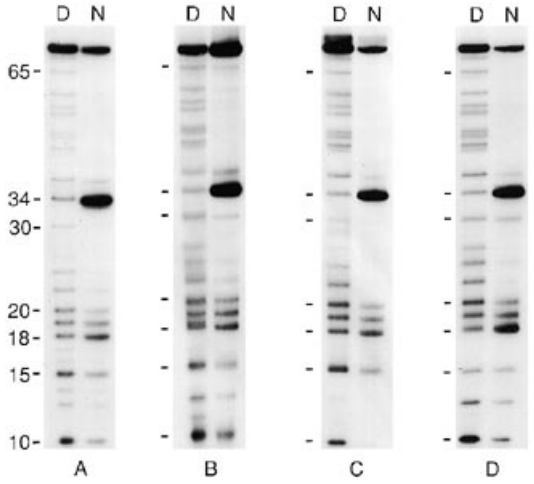

Figure 2. RNase T1 analysis of 5′-^{32}P-end-labeled tRNAs. (**A**) Unmodified tRNA^{Phe}; (**B**) $\mathbf{I_{XL}}$; (**C**) $\mathbf{II_{XL}}$; (**D**) $\mathbf{III_{XL}}$. Cleavage reactions were conducted in 10 mM Tris–HCl, 200 mM NaCl, pH 7.0, at 25°C under both denaturing (D, 7.4 M urea, no Mg^{2+}) and native (N, 15 mM $MgCl_2$) conditions.

The RNase T1 cleavage intensities observed under native conditions are nearly identical for all three cross-linked tRNAs and are very similar to that observed for unmodified yeast tRNA^{Phe} (Fig. 2). In addition, the t-butyl disulfide-modified tRNAs each show the same cleavage pattern/intensity under these conditions (data not shown). For all of the sequences hypercleavage is observed at G34 (35–40% of the fragments obtained under 'single-cut' conditions) and minor cleavage is observed at G37. Residue G20 is not involved in tertiary interactions and should be more accessible to cleavage than residues G18 and G19. However, while cleavage at G20 is observed for all sequences, the intensity of cleavage is lower than that observed for G18 and G19. Similar cleavage profiles have been reported for yeast tRNA^{Phe} (42).

Residue G15 is involved in reverse Watson–Crick pairing with C48 and cleavage at this position is observed in all cases, with a 2% reduction in relative intensity for cleavage in $\mathbf{III_{XL}}$ relative to the other sequences. Reduced cleavage here is also observed under denaturing conditions, which suggests that the alkylthiol linker on $\mathbf{U^{2'S}16}$ may sterically interfere with enzyme activity. Minor cleavage (<2% of all cleavage products) is observed at D stem residues G22 and G24 for each of the cross-linked tRNAs, the t-butyl disulfide-modified tRNAs and for the parent sequence. There are no reports of cleavage at these positions for folded native yeast tRNA^{Phe}. These observations indicate that there may be structural or dynamic differences in this region of both unmodified tRNA^{Phe} and our disulfide-modified constructs compared to native yeast tRNA^{Phe}. However, the absence of cleavage at guanosine residues involved in base pairing and known tertiary interactions, including residues in base pairs proximal to the cross-links (i.e. C2·G71 for $\mathbf{I_{XL}}$; C27·G43 for $\mathbf{II_{XL}}$; C61·G53 for $\mathbf{III_{XL}}$), indicates that within the resolution of this assay our modifications do not significantly alter the global structure of unmodified yeast tRNA^{Phe}.

We next probed the D-loop/T-loop interface which forms the characteristic shape of folded tRNAs. When the D-loop and T-loop are properly positioned, formation of a cyclobutane dimer between residues C48 and U59 can be induced by irradiation at 254 nm (33). Behlen *et al.* have shown that comparing the rate of formation of this photoproduct for unmodified yeast tRNA^{Phe} with mutant tRNAs can be indicative of proper tertiary structure (33). For all of the thiol-modified sequences, with the exception of $\mathbf{III_{tBu}}$, the rates of cyclobutane dimer formation are within 80% of the rate for unmodified yeast tRNA^{Phe} (Table 1). The rate of ultraviolet cross-link formation for $\mathbf{III_{tBu}}$ is 2-fold lower than the rate of cross-link formation for unmodified yeast tRNA^{Phe}, which suggests that $\mathbf{III_{tBu}}$ may possess a destabilized, incomplete or distorted tertiary structure. However, removal of the t-butyl protecting groups on $\mathbf{III_{tBu}}$ and formation of the disulfide cross-link ($\mathbf{III_{XL}}$) restores the rate of cross-link formation to the same level as unmodified yeast tRNA^{Phe}. Taken together the results of these experiments suggest that our cross-links do not significantly disrupt the positioning of residues C48 and U59 within the hinge region of the folded tRNA.

Perhaps the most sensitive probe of the hinge region created by interaction of the D loop and the T loop is the rate of Pb^{2+}-induced autocleavage (40). Pb(II) binds to yeast tRNA^{Phe} by specifically contacting functional groups on bases U59 and C60, as well as the phosphate of G19 (43). Under suitable conditions of temperature and pH a lead atom bound to these bases causes specific hydrolysis of the phosphodiester bond between residues U17 and G18 in properly folded yeast tRNA^{Phe} (43). When the native tertiary structure is not present only non-specific hydrolysis is observed. Specific hydrolysis between residues U17 and G18 also occurs for unmodified yeast tRNA^{Phe} and the rate of this reaction can decrease when the tertiary structure is not correctly formed (40).

Table 1. Rates of ultraviolet cross-link formation and Pb^{2+} cleavage

Sequence	Cross-linking rate (per min × 10^2)	Relative cross-linking rate	Pb^{2+} cleavage rate (per s × 10^4)	Relative Pb^{2+} cleavage rate
Unmodified	4.6 ± 0.1	1.0	5.57 ± 0.08	1.0
$\mathbf{I_{tBu}}$	3.8 ± 0.4	0.83	7.3 ± 1.2	1.3
$\mathbf{I_{XL}}$	3.8 ± 0.4	0.83	5.5 ± 0.3	0.99
$\mathbf{II_{tBu}}$	4.2 ± 0.4	0.91	3.3 ± 0.6	0.59
$\mathbf{II_{XL}}$	4.4 ± 0.2	0.96	5.8 ± 0.4	1.0
$\mathbf{III_{tBu}}$	2.6 ± 0.3	0.57	0.58 ± 0.02	0.1
$\mathbf{III_{XL}}$	3.7 ± 0.4	0.80	[a]–	[a]–

Rates are obtained from the first 5 min exposure to 254 nm irradiation and from the first 8 min incubation with Pb^{2+}. Errors represent one standard deviation from two to six individual determinations.
[a]Pb^{2+} cleavage not observed.

Table 2. T_m values (°C) and van't Hoff thermodynamic data from optical melting experiments

Sequence	T_m[a,c]	Hyperchromicity (%)[a,d]	T_m[b,c]	ΔH_{VH}[b,c]	ΔS_{VH}[b,c]	ΔG_{VH}[b,c]	Hyperchromicity (%)[b,d]
Unmodified yeast tRNA^{Phe}	54.0 ± 0.6	25	69 ± 1	–44 ± 3	–131 ± 8	–5.7 ± 0.3	27
$\mathbf{I_{tBu}}$	60.1 ± 0.9	22	70 ± 1	–41 ± 4	–120 ± 13	–5.2 ± 0.4	24
$\mathbf{I_{XL}}$	58.0 ± 0.2	26	70.2 ± 0.3	–38.4 ± 0.3	–112 ± 1	–5.0 ± 0.1	26
$\mathbf{II_{tBu}}$	53.0 ± 0.6	22	69.2 ± 0.3	–42 ± 2	–123 ± 7	–5.5 ± 0.4	23
$\mathbf{II_{XL}}$	52.8 ± 0.1	23	68 ± 3	–48 ± 7	–140 ± 21	–5.9 ± 0.6	22

[a]10 mM Na cacodylate, 90 mM NaCl, pH 6.8.

[b]10 mM Na cacodylate, 90 mM NaCl, 5 mM $MgCl_2$, pH 6.8.

[c]T_m values are in °C; ΔH_{VH} and ΔG_{VH} values are in kcal/mol; ΔS_{VH} values are in eu. Errors represent one standard deviation from two to five replicates of the experiment.

[d]Errors are ±3%. In both the presence and absence of Mg^{2+} the shapes of the melting curves for each modified construct are similar to the shape of the melting profile for unmodified tRNA^{Phe}, suggesting that the modifications do not substantially alter the denaturation pathway of the tRNA. Also, the hyperchromicity changes for the cross-linked constructs are within the error of those measured for unmodified yeast tRNA^{Phe}, which indicates that the denatured states of the cross-linked tRNAs are similar to unmodified yeast tRNA^{Phe} with respect to base stacking (9).

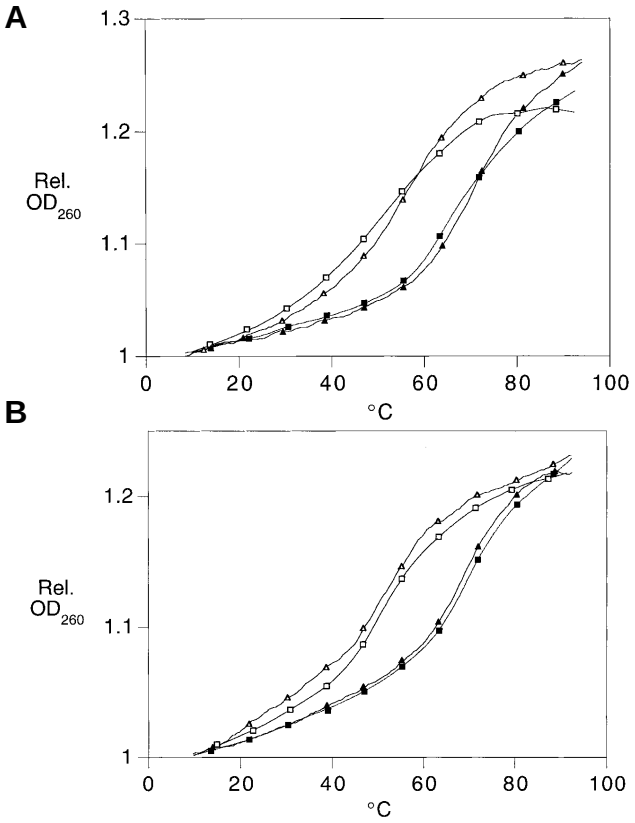

Figure 3. Representative normalized UV thermal denaturation curves. (**A**) Site **I** measured in 10 mM Na cacocylate, 90 mM NaCl, pH 6.8: $\mathbf{I_{tBu}}$ (□); $\mathbf{I_{XL}}$ (△); $\mathbf{I_{tBu}}$ + 5 mM Mg^{2+} (■); $\mathbf{I_{XL}}$ + 5 mM Mg^{2+} (◆); (**B**) site **II** obtained in 10 mM Na cacocylate, 90 mM NaCl, pH 6.8: $\mathbf{II_{tBu}}$ (□); $\mathbf{II_{XL}}$ (△); $\mathbf{II_{tBu}}$ + 5 mM Mg^{2+} (■); $\mathbf{II_{XL}}$ + 5 mM Mg^{2+} (◆).

The rates of Pb^{2+}-catalyzed cleavage for both $\mathbf{I_{XL}}$ and $\mathbf{II_{XL}}$ are within the error of that observed for unmodified yeast tRNA^{Phe} (Table 1). However, specific hydrolysis of $\mathbf{III_{XL}}$ is not observed. Since the RNase T1 footprinting and UV cross-linking results for this sequence indicate that the native tertiary structure does form, the lack of cleavage must originate from another factor. Positioning of the Pb(II) atom into a model of $\mathbf{III_{XL}}$ (43) shows that the cross-link spans the lead binding site. Therefore, we propose that the lack of hydrolysis of $\mathbf{III_{XL}}$ is more consistent with occlusion of the Pb^{2+} from the binding site by the cross-link rather than the result of a major structural perurbation. Thus, within the resolution of the solution probing experiments described above, we conclude that all three cross-linked tRNAs fold in the same manner as unmodified yeast tRNA^{Phe}.

Thermal denaturation

To examine the effect that the cross-links exert on the thermal stability of tRNA structure we recorded optical melting profiles of $\mathbf{I_{XL}}$ and $\mathbf{II_{XL}}$ along with their t-butyl disulfide-protected precursors (Fig. 3). In 100 mM Na^+ buffer (conditions where only secondary structure forms), substitution of G1·C72 in $\mathbf{I_{tBu}}$ stabilizes the tRNA by 6°C relative to unmodified yeast tRNA^{Phe} (Table 2). Since our modification removes the possibility for base pairing, the increase in melting temperature (T_m) for this transition from folded tRNA to random coil probably originates from another favorable factor, like Van der Waals interactions between the t-butyl groups and alkyl linkers present on $\mathbf{U^{3S}}$. Such effects have been observed in other systems possessing this modification (44).

Placing a cross-link at the acceptor stem terminus ($\mathbf{I_{XL}}$) results in a 4°C increase in T_m relative to unmodified yeast tRNA^{Phe}. In contrast, $\mathbf{II_{XL}}$ does not afford an increase in T_m relative to either $\mathbf{II_{tBu}}$ or unmodified tRNA^{Phe}. At first this result is somewhat surprising, given that the denatured state of $\mathbf{II_{XL}}$ should be entropically destabilized relative either to $\mathbf{II_{tBu}}$ or unmodified yeast tRNA^{Phe} (45). However, the T_m for the overall melting transition to a coil for a cross-linked tRNA can differ from the parent tRNA if the disulfide bond links structural elements that unfold prior to the overall T_m. The acceptor stem of yeast tRNA^{Phe} melts prior to the overall T_m of unfolding in both low and high salt buffers (46,47). Given the high sequence similarity of the helical stems of yeast tRNA^{Phe} and unmodified yeast tRNA^{Phe}, the thermal stabilities of these stems should be similar. Thus we propose that the increase in T_m observed for $\mathbf{I_{XL}}$ arises because the acceptor stem is stabilized by the disulfide bond, whereas the absence of an effect of the disulfide bond on the T_m of $\mathbf{II_{XL}}$ results because the D-stem denatures late in the thermal unfolding pathway (47).

In buffers containing Mg^{2+}, unmodified yeast tRNA^{Phe} adopts the proper tertiary structure and the T_m values for the t-butyl disulfide-modified tRNAs ($\mathbf{I_{tBu}}$, $\mathbf{II_{tBu}}$) and their cross-linked counterparts ($\mathbf{I_{XL}}$, $\mathbf{II_{XL}}$) are within the error of the value for unmodified yeast tRNA^{Phe} (Table 2). These results suggest that our modifications do not destabilize the tRNA, in agreement with the footprinting data obtained for these constructs. The large increase in thermal stability that occurs upon addition of Mg^{2+} to the cross-linked tRNAs compared with the small increase that occurs as a result of introducing one disulfide cross-link demonstrates that a single disulfide bond cannot substitute for Mg^{2+} in stabilizing the

folded tRNA structure. Assuming that in the presence of Mg^{2+} denaturation proceeds in a two-state manner (46; i.e. melting of the properly folded tRNA directly to a coil), van't Hoff analysis suggests that there are compensating enthalpic and entropic effects which result in similar T_m and ΔG_{VH} values for each of the modified tRNAs (Table 2). Though we are unable to precisely determine the source of the entropic and enthalpic effects from these data alone (i.e. a non-native disulfide bond can lead to differential solvation or ion binding; see 9), we can conclude that our alkylthiol modifications and corresponding cross-links do not destabilize the tRNA.

In summary, we have demonstrated that disulfide cross-links can be site specifically incorporated into unmodified yeast $tRNA^{Phe}$ and that cross-link formation between thiol-derivatized loci correlates with the position of these groups in the crystal structure of yeast $tRNA^{Phe}$. Each of the thiol-modified tRNAs was synthesized in high yield and in each case cross-link formation was quantitative. In this regard our disulfide cross-link chemistry compares very favorably with other methods for introducing cross-links within RNA (33,48,49). With the work described here, synthesis of each of the four RNA bases derivatized with 2′-*O*-alkyl linkers has been completed (23,50–52). In addition to these monomers, alkylthiol-modified nucleosides have been described with linkers at, among others, the C5 position of pyrimidines (53), the C8 position of purines (50) and at all exocyclic amine groups on both purines and pyrimidines (27). Thus it should be possible to selectively form a cross-link between any two positions on an RNA. By analogy to the host of experiments devised for proteins containing native and engineered cysteine residues, the ability to place thiol groups and disulfide cross-links at specified positions within RNA should facilitate examination of the structure, conformational flexibility, dynamics, folding pathways and biological activity of ribonucleic acids. The results of our efforts in each of these areas will be reported shortly.

REFERENCES

1 Creighton,T.E. (1992) *Protein Folding.* W.H.Freeman and Co., New York, NY.
2 Tinoco,I.,Jr, Puglisi,J.D. and Wyatt,J.R. (1990) *Prog. Nucleic Acid Mol. Biol.*, **4**, 205–226.
3 Draper,D.E. (1996) *Trends Biochem. Sci.*, **21**, 145–149.
4 Thirumalai,D. and Woodson,S.A. (1996) *Acc. Chem. Res.*, **29**, 433–439.
5 Doudna,J.A. and Cate,J.H. (1997) *Curr. Opin. Struct. Biol.*, **7**, 310–316.
6 Cech,T.R. (1993) *Biochem. Soc. Trans.*, **21**, 229–234.
7 Clarke,J. and Fersht,A.R. (1993) *Biochemistry*, **32**, 4322–4329.
8 Falke,J.J. and Koshland,D.E.,Jr (1994) *Science*, **237**, 1596–1600.
9 Vslker,J., Osborne,S.E., Glick,G.D. and Breslauer,K.J. (1997) *Biochemistry*, **36**, 756–767.
10 Osborne,S.E., Cain,R.J. and Glick,G.D. (1997) *J. Am. Chem. Soc.*, **119**, 1171–1182.
11 Cain,R.J. and Glick,G.D. (1997) *Nucleic Acids Res.*, **25**, 836–842.
12 Erlanson,D.A., Glover,J.N.M. and Verdine,G.L. (1997) *J. Am. Chem. Soc.*, **119**, 6927–6928.
13 Osborne,S.E., Völker,J., Stevens,S.Y., Breslauer,K.J. and Glick,G.D. (1996) *J. Am. Chem. Soc.*, **118**, 11993–12003.
14 Cain,R.J., Zuiderweg,E.R.P. and Glick,G.D. (1995) *Nucleic Acids Res.*, **23**, 2153–2160.
15 Ferentz,A.E., Keating,T.A. and Verdine,G.L. (1993) *J. Am. Chem. Soc.*, **115**, 9006–9014.
16 Wang,H., Osborne,S.E., Zuiderweg,E.R.P. and Glick,G.D. (1994) *J. Am. Chem. Soc.*, **116**, 5021–5022.
17 Wolfe,S.A. and Verdine,G.L. (1993) *J. Am. Chem. Soc.*, **115**, 12585–12586.
18 Glick,G.D., Osborne,S.E., Knitt,D.S. and Marino,J.P.,Jr (1992) *J. Am. Chem. Soc.*, **114**, 5447–5448.
19 Stevens,S.Y., Swanson,P.C., Voss,E.W.,Jr and Glick,G.D. (1993) *J. Am. Chem. Soc.*, **115**, 1585–1586.
20 Erlanson,D.A., Chen,L. and Verdine,G.L. (1993) *J. Am. Chem. Soc.*, **115**, 12583–12584.
21 Chaudhuri,N.C. and Kool,E.T. (1995) *J. Am. Chem. Soc.*, **117**, 10434–10442.
22 Goodwin,J.T. and Glick,G.D. (1994) *Tetrahedron Lett.*, **35**, 1647–1650.
23 Goodwin,J.T., Osborne,S.E., Scholle,E.J. and Glick,G.D. (1996) *J. Am. Chem. Soc.*, **118**, 5207–5215.
24 Sigurdsson,S.Th., Tuschl,T. and Eckstein,F. (1995) *RNA*, **1**, 575–583.
25 Allerson,C.R. and Verdine,G.L. (1995) *Chem. Biol.*, **2**, 667–675.
26 Cohen,S.B. and Cech,T.R. (1997) *J. Am. Chem. Soc.*, **119**, 6259–6268.
27 Allerson,C.R., Chen,S.L. and Verdine,G.L. (1997) *J. Am. Chem. Soc.*, **119**, 7423–7433.
28 Sproat,B.S., Iribarren,A., Beijer,B., Pieles,U. and Lamond,A.I. (1991) *Nucleosides Nucleotides*, **10**, 25–36.
29 Wünsch,E., Moroder,L. and Romani,S. (1982) *Hoppe-Seyler's Z. Physiol. Chem.*, **363**, 1461–1464.
30 Parvari,R., Pecht,I. and Soreq,H. (1983) *Anal. Biochem.*, **133**, 450–456.
31 Hall,K.B. and Sampson,J.R. (1990) *Nucleic Acids Res.*, **18**, 7041–7047.
32 Han,H. and Dervan,P.B. (1994) *Proc. Natl. Acad. Sci. USA*, **91**, 4955–4959.
33 Behlen,L.S., Sampson,J.R. and Uhlenbeck,O.C. (1992) *Nucleic Acids Res.*, **20**, 4055–4059.
34 Rigler,R. and Wintermeyer,W. (1983) *Annu. Rev. Biophys. Bioengng*, **12**, 475–505.
35 Scaringe,S.A., Francklyn,C. and Usman,N. (1990) *Nucleic Acids Res.*, **18**, 5433–5441.
36 Gasparutto,D., Livache,T., Bazin,H., Duplaa,A.-M., Guy,A., Khorlin,A., Molko,D., Roget,A. and Téoule,R. (1992) *Nucleic Acids Res.*, **20**, 5159–5166.
37 Ogilvie,K.K., Usman,N., Nicoghosian,K. and Cedergren,R.J. (1988) *Proc. Natl. Acad. Sci. USA*, **85**, 5764–5768.
38 Ellman,G.L. (1959) *Arch. Biochem. Biophys.*, **82**, 70–77.
39 Siggurdsson,S.Th. and Eckstein,F. (1996) *Anal. Biochem.*, **235**, 241–242.
40 Behlen,L.S., Sampson,J.R., DiRenzo,A.B. and Uhlenbeck,O.C. (1990) *Biochemistry*, **29**, 2515–2523.
41 Ehresmann,C., Baudin,F., Mougel,M., Romby,P., Ebel,J.-P. and Ehresmann,B. (1987) *Nucleic Acids Res.*, **15**, 9109–9128.
42 Wrede,P., Wurst,R., Vournakis,J. and Rich,A. (1979) *J. Biol. Chem.*, **254**, 9608–9616.
43 Brown,R.S., Dewan,J.C. and Klug,A. (1985) *Biochemistry*, **24**, 4785–4801.
44 Osborne,S.E. (1996) PhD Thesis, University of Michigan.
45 Poland,D.C. and Scheraga,H.A. (1965) *Biopolymers*, **3**, 379–399.
46 Privalov,P.L. and Filimonov,V.V. (1978) *J. Mol. Biol.*, **122**, 447–464.
47 Coutts,S.M., Riesner,D., Rsmer,R., Rabl,C.R. and Maass,G. (1975) *Biophys. Chem.*, **3**, 275–289.
48 Harris,M.E., Nolan,J.M., Malhotra,A., Brown,J.W., Harvey,S.C. and Pace,N.R. (1994) *EMBO J.*, **13**, 3953–3963.
49 Branch,A.D., Benenfeld,B.J., Paul,C.P. and Robertson,H.D. (1989) *Methods Enzymol.*, **180**, 418–442.
50 Gundlach,C.W., Ryder,T.R. and Glick,G.D. (1997) *Tetrahedron Lett.*, **38**, 4039–4042.
51 Douglas,M.E., Beijer,B. and Sproat,B.S. (1994) *Bioorg. Med. Chem. Lett.*, **4**, 995–1000.
52 Manoharan,M., Johnson,L.K., Tivel,K.L., Springer,R.H. and Cook,P.D. (1993) *Bioorg. Med. Chem. Lett.*, **3**, 2765–2770.
53 Sun,S., Tang,X.-Q., Merchant,A., Anjaneyulu,P.S.R. and Piccirilli,J.A. (1996) *J. Org. Chem.*, **61**, 5708–5709.